

Sensory and Motor Systems

# Individualized Assays of Temporal Coding in the Ascending Human Auditory System

Agudemu Borjigin,<sup>1</sup> Alexandra R. Hustedt-Mai,<sup>2</sup> and Hari M. Bharadwaj<sup>1,2</sup><https://doi.org/10.1523/ENEURO.0378-21.2022><sup>1</sup>Weldon School of Biomedical Engineering, Purdue University, West Lafayette, IN and <sup>2</sup>Department of Speech, Language, and Hearing Sciences, Purdue University, West Lafayette, IN 47907

## Abstract

Neural phase-locking to temporal fluctuations is a fundamental and unique mechanism by which acoustic information is encoded by the auditory system. The perceptual role of this metabolically expensive mechanism, the neural phase-locking to temporal fine structure (TFS) in particular, is debated. Although hypothesized, it is unclear whether auditory perceptual deficits in certain clinical populations are attributable to deficits in TFS coding. Efforts to uncover the role of TFS have been impeded by the fact that there are no established assays for quantifying the fidelity of TFS coding at the individual level. While many candidates have been proposed, for an assay to be useful, it should not only intrinsically depend on TFS coding, but should also have the property that individual differences in the assay reflect TFS coding per se over and beyond other sources of variance. Here, we evaluate a range of behavioral and electroencephalogram (EEG)-based measures as candidate individualized measures of TFS sensitivity. Our comparisons of behavioral and EEG-based metrics suggest that extraneous variables dominate both behavioral scores and EEG amplitude metrics, rendering them ineffective. After adjusting behavioral scores using lapse rates, and extracting latency or percent-growth metrics from EEG, interaural timing sensitivity measures exhibit robust behavior-EEG correlations. Together with the fact that unambiguous theoretical links can be made relating binaural measures and phase-locking to TFS, our results suggest that these “adjusted” binaural assays may be well suited for quantifying individual TFS processing.

**Key words:** electroencephalography; frequency modulation; interaural time difference; neural coding; nonsensory factors; temporal fine structure

## Significance Statement

The auditory system is unique among the senses in that neurons in the periphery fire precisely phase-locked spikes in response to fast temporal fluctuations in sound. Yet, the functional significance of this metabolically expensive neural code is debated. Here, we establish behavioral and physiological assays that can probe the fidelity of this phase-locking mechanism at the level of individual human subjects. These measures pave the way for future experiments that can more directly address foundational questions about the role of phase locking in everyday hearing, and test whether phase-locking deficits contribute to the listening difficulties in clinical populations. Importantly, our results also show that commonly used measures to assess phase locking are affected by extraneous variables, and thus ineffective.

## Introduction

All acoustic information we receive is conveyed through the firing rate and/or timing of the neural spikes (i.e., rate-place vs temporal coding) of cochlear neurons. Temporal

information in the basilar-membrane vibrations consists of cycle-by-cycle variations in phase, the temporal fine structure (TFS), and dynamic variations in amplitude, the envelope (ENV; Hilbert, 1906). Cochlear neurons phase-

Received September 16, 2021; accepted February 8, 2022; First published February 22, 2022.

The authors declare no competing financial interests.

Author contributions: A.B. and H.M.B. designed research; A.B. and A.R.H.-M. performed research; A.B. and H.M.B. analyzed data; A.B., A.R.H.-M., and H.M.B. wrote the paper.

lock to both TFS (Johnson, 1980), and ENV (Joris and Yin, 1992) robustly, with TFS phase-locking extending at least up to 1000 Hz (Verschooten et al., 2019). While the peripheral rate-place code has consistent counterparts throughout the auditory system, the upper limit of phase-locking progressively shifts to lower frequencies along the ascending pathway (Joris et al., 2004). How this metabolically expensive initial/peripheral temporal code (Laughlin et al., 1998; Hasenstaub et al., 2010) contributes to everyday hearing and how its degradation contributes to perceptual deficits are foundational questions in auditory neuroscience and clinical audiology. Yet, the significance of TFS coding is debated (Drullman, 1995; Oxenham and Simonson, 2009; Swaminathan and Heinz, 2012; Oxenham, 2013).

Previous studies have explored whether sound localization and pitch perception benefit from TFS cues. While it is established that lateralization of low-frequency sounds depends on TFS (Smith et al., 2002; Yin and Chan, 1990), whether TFS is important for pitch perception is difficult to ascertain. Behavioral studies suggest that low-frequency periodic sounds elicit a stronger pitch than high-frequency sounds (Moore, 1973; Houtsma and Smurzynski, 1990; Bernstein and Oxenham, 2003), suggesting a possible role for TFS. However, these results permit alternate interpretations in terms of place coding and harmonic resolvability (Oxenham, 2012). Regardless of its role in quiet, whether TFS is important for masking release in noise is further debated, especially when other redundant cues can also convey pitch or location, and when room reverberation can degrade temporal cues (Best et al., 2005; Oxenham and Simonson, 2009; Ihlefeld and Shinn-Cunningham, 2011).

To investigate the role of TFS, studies have used sub-band vocoding to independently manipulate ENV and TFS cues (Smith et al., 2002; Hopkins et al., 2008; Hopkins and Moore, 2009; Lorenzi et al., 2009; Ardoit and Lorenzi, 2010). However, acoustic manipulations cannot eliminate subsequent confounding of ENV, TFS, and place cues without detailed knowledge of cochlear processing at the individual level (Swaminathan and Heinz, 2012; Oxenham, 2013). Thus, establishing the precise role of TFS through vocoding experiments is difficult, although the use of high-fidelity vocoders can help (Viswanathan et al., 2021). An alternative approach is to directly measure TFS sensitivity from individual listeners and compare it to individual differences in other perceptual measures. The individual-differences approach has been successfully used to address other fundamental questions (McDermott et al., 2010; Bharadwaj et al., 2015; Whiteford

et al., 2020). Unfortunately, the lack of established measures of TFS sensitivity at the individual level limits this enterprise.

Conventional behavioral TFS-sensitivity measurements have attempted to eliminate confounding cues such that primary task would rely on TFS processing (Strelcyk and Dau, 2009; Moore and Sek, 2009; Hopkins and Moore, 2010; Sek and Moore, 2012). However, they did not assess the influence of extraneous factors on the measured scores. Unfortunately, nonsensory factors can contribute significantly to individual variability even when the tasks themselves rely on specific acoustic cues (Kidd et al., 2007). Objective electrophysiological measures of TFS sensitivity can circumnavigate this problem; however, such studies are scarce (Verschooten et al., 2015; Parthasarathy et al., 2020). Here, we employ a battery of both behavioral and electroencephalography (EEG)-based measures of TFS sensitivity on a cohort of normal-hearing (NH) individuals to identify candidate assays of TFS processing at the individual level. Our results suggest that extraneous variables dominate both behavioral and raw EEG measures. However, with adjustments, we observed robust behavior-EEG correlations in binaural assays, rendering them well suited for quantifying individual TFS processing.

## Materials and Methods

The primary goal of the current study was to evaluate an array of both behavioral and electrophysiological measures as candidate assays of TFS sensitivity at the individual level. Based on the finding that nonsensory factors contribute significantly to behavioral TFS measures, a large-N supplementary behavioral experiment was conducted to assess whether nonsensory factors also influence ENV sensitivity when measured from naive participants.

## Participants

One hundred and fifty-three listeners, aged 18–60 years, were recruited from the local community near Purdue University. All human subject measures were conducted following protocols approved by the Purdue University Internal Review Board and the Human Research Protection Program. Participants were recruited via posted flyers and bulletin-board advertisements and provided informed consent. All participants had pure-tone air-conduction thresholds of 25 dB Hearing Level (HL) or better at octave frequencies from 500 to 8000 Hz. Of the 153 subjects, 44 (20 males) participated in the main experiments designed to evaluate candidate assays of TFS processing. The remaining  $N = 109$  participated in the supplementary experiment aimed at testing whether nonsensory factors also influence ENV sensitivity. Although the goal of the main experiment was to conduct all behavioral and electrophysiological TFS measures on each participant, some were not able to finish the full study battery because of limited availability. Among the 44 listeners who participated in the main study, 43 completed the frequency modulation (FM) detection task, and 36 completed the interaural time difference (ITD) detection task. The intersection, 33 subjects, completed both behavioral measurements. Among all participants ( $n = 44$ ), 42 subjects

This work was supported by the National Institutes of Health Grant R01DC015989.

Correspondence should be addressed to Hari M. Bharadwaj at [hbharadwaj@purdue.edu](mailto:hbharadwaj@purdue.edu).

<https://doi.org/10.1523/ENEURO.0378-21.2022>

Copyright © 2022 Borjigin et al.

This is an open-access article distributed under the terms of the Creative Commons Attribution 4.0 International license, which permits unrestricted use, distribution and reproduction in any medium provided that the original work is properly attributed.

completed EEG-ITD sensitivity measurements; 25 of those 42 subjects also completed EEG-frequency following response (FFR) measurements. Among the subjects who completed both behavioral measurements, all except one ( $n=32$ ) completed the EEG-ITD measurement; these subjects include all participants who completed the EEG-FFR measurements ( $n=25$ ). The subjects who completed both behavioral measurements ( $n=32$ , age: mean = 26.8, SD = 11.2) were included for the main analyses including brain-behavior correlations. Although the age range was wide, only six out of 33 subjects were older than 35 years at the time of the testing, and age did not significantly correlate with any measure of this study.

## Experimental design and statistical analyses

### *Behavioral measures of the TFS coding*

Each of the following behavioral measurements was conducted on a different day from the others to randomize the influence of factors that may be idiosyncratic to a specific test day/session. A single lab visit contained only one behavioral measurement to reduce the impact of cognitive fatigue from hour-long experiments.

**FM detection thresholds.** To obtain monaural TFS sensitivity, FM thresholds were measured separately in each ear, using a weighted (3:1) one-down-one-up (Kaernbach, 1991), two-alternatives-forced-choice (2AFC) adaptive procedure. The stimulus in the target interval was a 500-ms-long 500-Hz tone with FM at a 2-Hz rate and variable depth. The reference interval was a 500-Hz pure tone. The interstimulus gap was 900 ms. The stimulus was ramped on and off with a rise/fall time of 5 ms to eliminate audible transitions. The stimulus level was 70 dB SPL. The subjects were instructed to press a button to indicate the interval containing the FM. Each measurement block was terminated after 11 reversals and the median of all the reversals from the adaptive procedure was extracted as the threshold. Four blocks of measurements were obtained in each ear from each subject. Except for an additional “demo” block to orient the participants before the formal testing, there was no further training. Sennheiser HDA 300 over-the-ear headphones were used for stimulus delivery. The slow FM rate of 2 Hz was chosen because it is thought that TFS cues are used to detect FM at rates below  $\sim 10$  Hz (Moore and Sek, 1996; Strelcyk and Dau, 2009). However, recent evidence suggests that this may not be the case (Whiteford et al., 2020). Nonetheless, given the large body of literature using and interpreting slow-FM detection as a measure of TFS sensitivity, we chose to include this in the battery of candidate measures.

**ITD detection thresholds.** To obtain a binaural measure of TFS sensitivity, we measured ITD detection thresholds using a three-down-one-up, 2AFC adaptive procedure. The stimulus consisted of two consecutive 400-ms-long, 500-Hz tone bursts with an ITD. The leading ear for the ITD was switched from the first burst to the second. The stimulus was ramped on and off with a rise/fall time of 20 ms to eliminate audible transitions and to reduce reliance on onset ITDs. The stimuli were presented at 70 dB

SPL. Subjects were asked to report the direction of the jump (left-to-right or right-to-left) between the intervals through a button press. It was preferable to have subjects indicate the direction of change because absolute lateralization can be influenced by multiple factors (Moore and Sek, 2009). The threshold was defined as the geometric mean of the last nine reversals, and measured repeatedly across eight blocks, with a short break scheduled after the fourth block. Etymotic Research (ER-2) insert earphones were used for delivering the stimuli. A separate “demo” block was included before the experimental blocks to familiarize the subject with the task.

**“Nonsensory” score.** Because the main goal of the study is to evaluate candidate measures of TFS coding in naive subjects, i.e., individuals without extensive training/practice on the measured tasks, we anticipated that extraneous “nonsensory” variables may influence the measured thresholds. Accordingly, percent-incorrect scores on easy “catch” trials were calculated to quantify the subject’s engagement. Errors made in these catch trials likely reflect nonsensory factors such as lapses in attention, variations in motivation, alertness, etc., rather than the strength of sensory coding. For the FM detection task, trials with frequency deviations (modulation depths)  $>15$  Hz were deemed to be catch trials, and the percent-incorrect scores were calculated for just these trials for each subject as an estimate of lapse rate. Similarly, the criterion for designating a trial as a “catch” trial for the ITD detection task was that the ITD exceeded  $80 \mu\text{s}$ . The number of catch trials available varied from subject to subject because of the adaptive nature of the task. On average, the FM and ITD detection tasks included 3–10 catch trials per block. To mitigate the influence of extraneous variables such as engagement and motivation on the measured thresholds, a simple linear model was constructed with this nonsensory score as the sole predictor, and the residuals from the model were treated as “clean” thresholds and used in all analyses thereafter.

**Supplementary amplitude modulation (AM) detection task.** To further investigate the influence of nonsensory factors on behavioral measures in general, we conducted a supplementary experiment using a task that is unrelated to TFS processing, an AM detection task similar to the one used in Bharadwaj et al. (2015). A similar 2AFC procedure as in the FM and ITD detection threshold measurements was employed. The target was a 500-Hz, 75 dB SPL band of noise centered at 4 or 8 kHz, and amplitude modulated at 19 Hz. Two unmodulated tones, flanked at two equivalent rectangular bandwidths (ERBs; Glasberg and Moore, 1990; Moore, 1986) away from the center frequency, each at 75 dB SPL, were used to minimize off-frequency listening. The signal in the reference interval was statistically identical but unmodulated. Using a noise carrier helps eliminate spectral cues for the AM detection task (Viemeister, 1979). The threshold for the modulation depth detection was determined by an adaptive weighted one-up-one-down procedure (Kaernbach, 1991).

### *Electrophysiological measures of TFS coding*

While behavioral measures directly assess perceptual sensitivity to TFS, they may also reflect common nonsensory factors such as attention and motivation. To dissociate TFS coding from nonsensory factors, we designed two passive EEG measures of TFS coding and compared them to individual behavioral measures. For EEG measurements, participants watched a silent, captioned video of their choice while passively listening to the auditory stimuli. EEG recordings were obtained using a 32-channel EEG system (Biosemi Active Two), while the stimuli were presented via ER-2 insert earphones.

**General EEG setup and preprocessing procedures.** The Biosemi EEG system employs active common-mode noise rejection using a pair of ground electrodes in a “driven-right leg” configuration (Metting van Rijn et al., 1990). EEG recordings were re-referenced to the average voltage across the two ear lobes. For cortical response analyses (EEG-ITD; see Cortical correlates of TFS-based ITD processing), the raw data were bandpass filtered from 1 to 50 Hz, whereas for subcortical responses (EEG-FFR; see FFR), raw data were filtered from 400 to 1300 Hz. The 400- to 1300-Hz bandpass filter eliminates artifacts from eye blinks. For the 1- to 50-Hz cortical data, ocular artifacts were removed using the signal-space projection technique (Uusitalo and Ilmoniemi, 1997). After the eye-blink correction, epochs with large voltage excursions (above 150  $\mu\text{V}$  for cortical recordings; above 50  $\mu\text{V}$  for subcortical recordings) were excluded to reduce movement artifacts. For both cortical and subcortical recordings, analyses focused on recordings from vertex electrodes (i.e., Fz and Cz channels).

**Cortical correlates of TFS-based ITD processing.** Cortical EEG was recorded in response to 70 dB SPL 500-Hz tones that were amplitude-modulated (100% depth) at 40.8 Hz. 40.8 Hz can elicit a strong auditory steady-state response (ASSR) in EEG recordings (Picton et al., 2003); this response was used here as a measure of recording quality (Fig. 1C). The stimulus duration was of 1.5 s. As with the behavioral measurement, the leading ear for the ITD switched 1 s into the trial. The direction of the ITD switch was randomized across trials. To minimize monaural cues, the ITD switch coincided with a trough of the 40.8 Hz modulation (Fig. 1A). This approach mirrors the method used in Papesch et al. (2017), where the stimulus switches between in-phase and out-of-phase states (phase shift of 180°). Our measurements involved ITD jumps of 20, 60, 180, or 540  $\mu\text{s}$  in magnitude. The magnitude and direction of the ITD jump were randomized across trials. A total of 1200 trials were presented to the listener. The interstimulus interval was uniformly distributed between 500 and 600 ms. Besides amplitude and latency of the averaged evoked response across trials in each condition, we calculated the intertrial coherence (ITC), which quantifies the consistency in the phase of the evoked response components across trials. ITC of 0 indicates no phase locking (the response is dominated by background noise), and ITC of 1 indicates perfect phase-consistency across trials (no background noise added to the phase-locked response). Thus, the ITC is directly

related to the signal-to-noise ratio of the evoked response (Bharadwaj and Shinn-Cunningham, 2014). The frequency band for ITC analysis was restricted to  $\sim 1$ –20 Hz, because it is known that cortical transient-evoked responses primarily consist of low-frequency components, and because we sought to separate these responses from the 40.8-Hz ASSR response.

**FFR.** Subcortical FFRs were measured in response to tones in a forward-masking stimulus configuration (Verschooten and Joris, 2014). The stimuli consisted of three consecutive segments: a 500-Hz probe tone that was 100 ms long and at 75 dB SPL, a “forward-masker” tone of the same frequency and duration but at 85 dB SPL, and the same probe tone. A 50-ms silent gap was included between the first probe tone and forward-masker, but only a 1-ms gap was included between the forward-masker and the second probe tone. Each stimulus segment was ramped on and off over 5 ms to reduce audible transitions. The polarity of the stimulus was alternated across a total of 8000 trials. The 500-Hz component of differential response obtained across the two stimulus polarities reflects response components that are phase-locked to the TFS, whereas the summed 500-Hz response represents the response to the ENV. However, the TFS component can contain both preneural (e.g., cochlear microphonic; CM) as well as neural responses. Verschooten and Joris (2014) argued that the nonlinear residual obtained by subtracting the TFS response to the second probe tone from the TFS response to the first probe tone will isolate the neural component and suppress the approximately linear CM. This is because the forward masking of response to the second probe tone only masks the neural component, whereas the CM is intact. Owing to the inner-hair-cell rectification, the summed response across the two polarities also contains a component at twice the stimulus frequency (1000 Hz) that reflects physiological currents phase-locked to the TFS in the stimulus. Although TFS-related, whether this double-frequency response is purely neural as has been previously interpreted (Parthasarathy et al., 2020), or whether it includes preneural contributions is unknown. Thus, we considered two candidate subcortical correlates of TFS processing: (1) the 500-Hz component derived from the differential response across the two polarities of stimulus presentation, and (2) the 1000-Hz component derived from the summed response across two polarities of stimulus presentation.

### *Statistical analyses*

Pearson correlations were calculated to illustrate simple associations between pairs of measurements. Statistical inference about behavior-physiology correlations was made using a multiple linear stepwise regression analysis by adding new potential predictors one by one to model the dependent variable. All reported significant associations met a false discovery rate criterion of 5% to control for multiple comparisons (Benjamini and Hochberg, 1995). Statistical analyses were performed using R (R Core Team, <https://www.r-project.org/>).

**Code accessibility.** Stimulus generation and data analyses were done using custom scripts. They can be accessed at: <https://github.com/AgudemuBorjigin/stimulus->

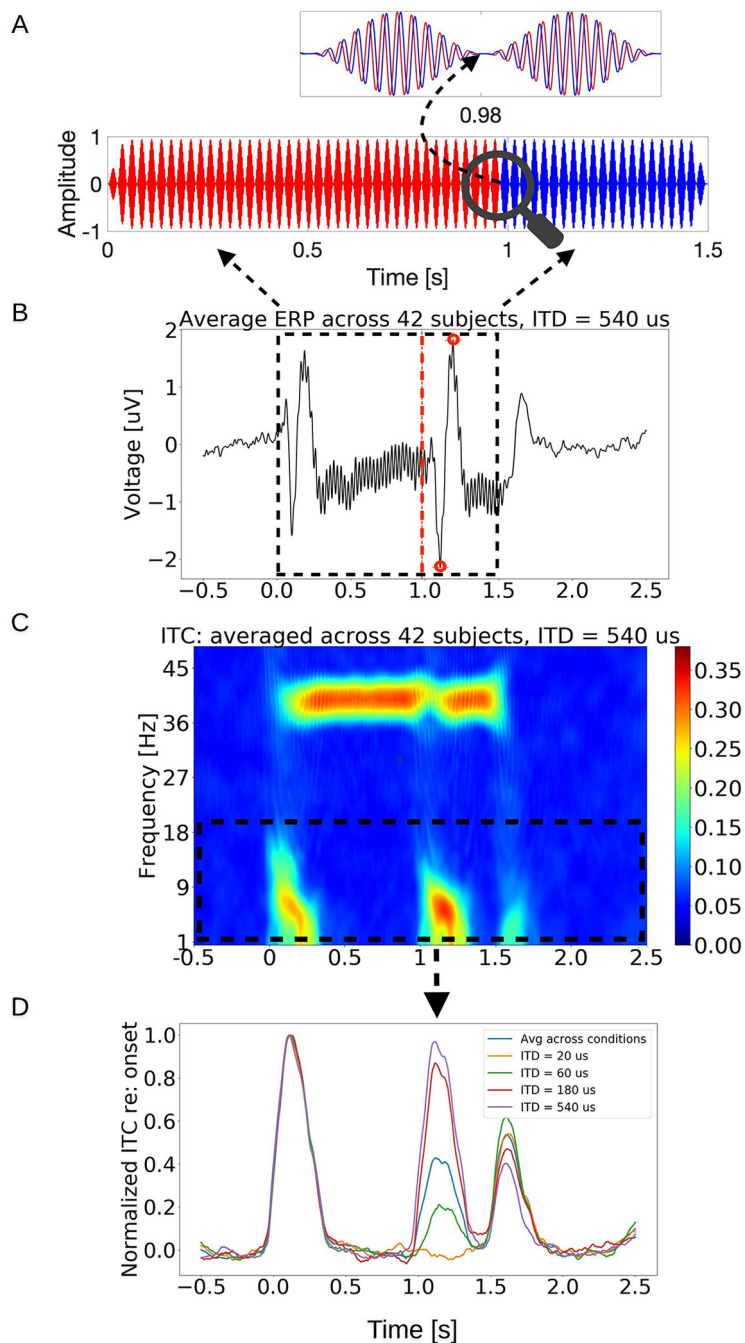


**Figure 1.** Stimulus paradigm and response from the EEG-TFS sensitivity measurement. **A**, The stimulus is a 1.5-s-long, 500-Hz pure tone that is amplitude modulated at 40.8 Hz. The red color represents the sound in the right ear, whereas the blue stands for the sound in the left ear. In the figure, the stimulus in the right ear leads in time till 0.98 s (indicated by the red segment of zoomed-out view of the stimulus), after which the ITD shifts in polarity, i.e., the stimulus in the left ear takes the lead. The ITD jump occurs when the stimulus amplitude is zero to minimize the involvement of monaural cues (pointed out by the dashed arrow). **B**, Averaged evoked response potential (ERP) from all trials across 42 subjects in “ITD = 540  $\mu$ s” condition from Cz electrode. The red dashed line indicates where the ITD switched polarity, which resulted in N1 and P2 responses (denoted by red dots). **C**, ITC spectrogram of the EEG response, averaged across 42 subjects, with the colormap indicating the ITC. Robust ASSRs can be seen around the AM frequency of 40.8 Hz. There are also salient responses time locked to the stimulus onset, offset, and importantly, to the ITD jump. **D**, The average time course of the ITC for frequencies below 20 Hz is shown for each ITD jump condition. The response evoked by the shift in the ITD polarity increases monotonically with the size of the ITD jump, confirming that the response is parametrically modulated by TFS-based processing.

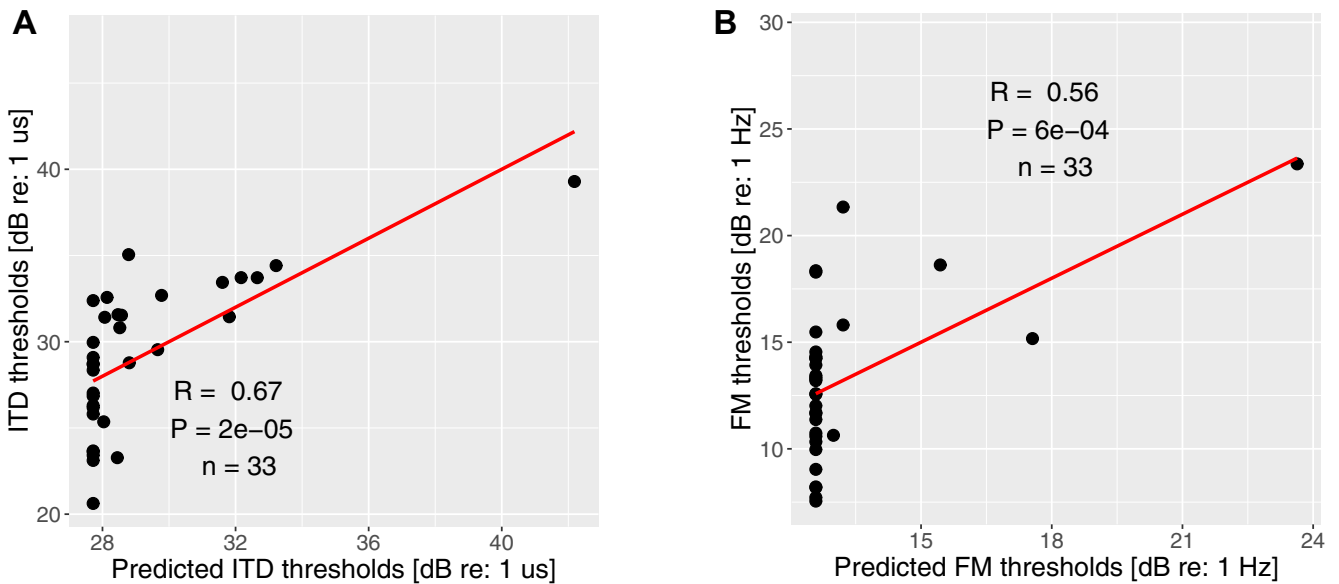


**Figure 2.** Measured versus predicted thresholds based on lapse rate. **A**, Measured versus predicted ITD detection thresholds. **B**, Measured versus predicted FM detection thresholds. The significant contribution of nonsensory factors is apparent, especially for the poorer performers.

TFS, <https://github.com/AgudemuBorjigin/EEGAnalysis>, and <https://github.com/AgudemuBorjigin/BehaviorDataAnalysis>.

## Results

### Nonsensory factors contribute to large individual differences in behavioral measures of TFS coding

Similar to previous reports of large individual differences in the AM and ENV-based ITD detection thresholds across NH listeners (Bharadwaj et al., 2015), both the FM and TFS-based ITD detection thresholds varied widely across our NH listeners. FM detection thresholds across 43 NH listeners ranged from 7 to 22 dB relative to 1 Hz [i.e., a frequency deviation (Fdev) of 2–13 Hz from 500 Hz]. ITD detection thresholds varied from 21 to 39 dB relative to 1  $\mu$ s (i.e., 11–89  $\mu$ s) across 37 NH listeners. These FM and ITD detection thresholds are shown along with the results from similar studies, in Figures 8 and 9, respectively, and were largely comparable.

Across listeners, neither FM (averaged across two ears) nor ITD thresholds (each averaged across repetitions) correlated with the audiograms (across-ear average of thresholds at 500 Hz; across-ear average of the mean thresholds at high frequencies: 4 and 8 kHz); however, the two measures were significantly correlated with each other in a simple linear regression analysis ( $r=0.44$ ,  $p=0.01$ ,  $n=33$ ). While the correlations may arise from individual differences in TFS coding, they can also reflect nonsensory factors such as attention, motivation, etc. To disambiguate these competing explanations, we assigned each listener a nonsensory score. When those scores were factored out from each measurement, the correlation between the monaural FM and binaural ITD thresholds dropped such that the association no longer met conventional statistical significance criteria ( $R=0.31$ ,

$p=0.08$ ,  $n=33$ ), suggesting that nonsensory factors play a large role in raw scores. Furthermore, when just the blocks with the largest (i.e., worst) FM and ITD thresholds for each subject were compared, considerably stronger correlations were observed ( $r=0.6$ ,  $p=9e-4$ ,  $n=33$ ), underscoring the involvement of nonsensory factors in behavioral measurements. Figure 2 shows the correlations between the measured and predicted thresholds solely based on the lapse rates (i.e., the nonsensory score). The involvement of nonsensory factors is evident, especially for the poorer performers.

To confirm the involvement of nonsensory factors in raw behavioral scores, a similar comparison of thresholds and lapse rates was conducted for the supplementary AM detection task. The predicted thresholds based on the nonsensory score significantly correlated with the measured AM thresholds ( $R=0.52$ ,  $p=1e-8$ ,  $n=109$ ; Fig. 3). This result indicates the significant weight of nonsensory factors, not only for FM and ITD detection measurements but behavioral measures in general.

### Raw electrophysiological TFS measures are strongly influenced by extraneous sources of variance

Two passive electrophysiological measurements were conducted to objectively evaluate individual TFS coding. Because passive electrophysiological measures are likely to be influenced by distinct extraneous factors (e.g., head size) compared with behavioral measures (e.g., motivation/engagement), these measurements provide a complementary window into individual TFS coding.

#### Candidate cortical correlates of TFS processing

Cortical responses evoked by the polarity shift of the ITD are quantified through the phase-locking strength shown in the phase-locking spectrograms (Fig. 1C). Clear

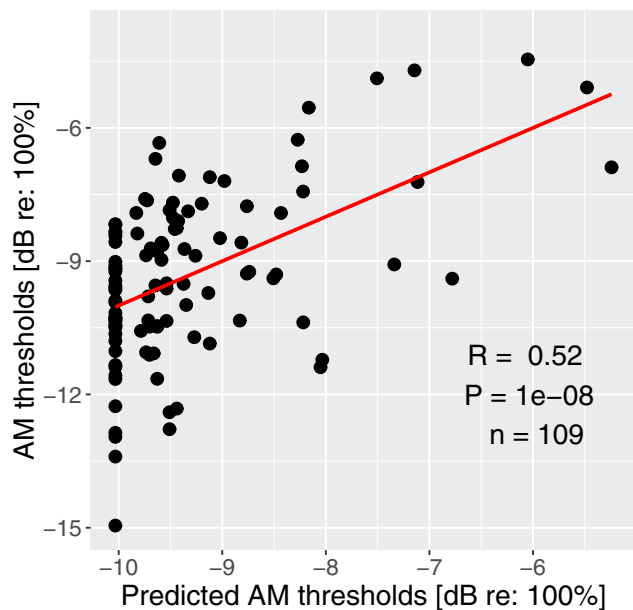


**Figure 3.** Measured versus predicted AM thresholds based on lapse rate. The thresholds are the average detection thresholds of AM tones at 4 and 8 kHz. The significant contribution of non-sensory factors is apparent.

responses to the onset, offset, and ITD jump are apparent in the low-frequency portion of the phase-locking spectrogram. The sustained ASSR is also clear around 40.8 Hz. The average response from 42 NH listeners shows monotonically increasing phase-locking strength of the ITD-evoked response across the ITD magnitudes (Fig. 1D), confirming that the response is indeed sensitive to TFS processing and the size of the ITD jump. Perhaps more important for the search of candidate TFS processing assays, large individual differences are apparent in the phase-locking strength across subjects (Fig. 4). Most subjects did not show a salient response for the 20- $\mu$ s condition, and only about half showed robust responses for the 60- $\mu$ s condition. Focusing therefore on the 180- and 540- $\mu$ s conditions, the 180- $\mu$ s condition is still part of the increasing slope of the response-versus-ITD-jump-size trend, but the response amplitude may have saturated for the 540  $\mu$ s. Accordingly, we used each individual's response for the 180- $\mu$ s condition for comparison to behavior. Note that the ITD being referred to here is the size of the jump; for instance, for the 20- $\mu$ s condition, the stimulus started with an ITD of 10  $\mu$ s with one ear leading and jumped to the other side about halfway through the stimulus to end with a 10- $\mu$ s ITD with the other ear leading.

Unfortunately, one striking aspect of the result in Figure 4 is that even at 540  $\mu$ s, the individual differences that were present in the lower ITD conditions persist. The ITD jump is obviously perceptible at 540  $\mu$ s, and the EEG response appears to be near saturation level for most individuals; this suggests that a significant portion of the individual differences in the magnitude of the cortical response arises from factors extraneous to TFS-based processing. Extraneous factors that may contribute

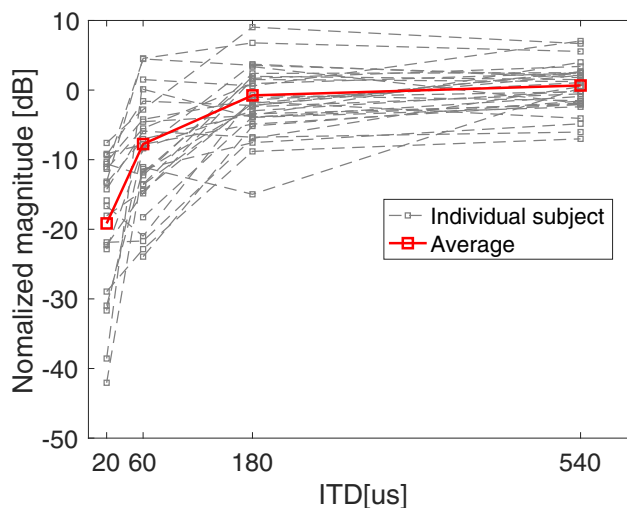


**Figure 4.** Individual EEG ITC (averaged under 20 Hz) values as a function of the jump size of the ITD. The ITC increases with the ITD for almost all subjects. Robust responses above noise floor are detected for most subjects for the “ITD = 180  $\mu$ s” condition. Interestingly, individual differences present at 180  $\mu$ s persist even at 540  $\mu$ s despite the ITD jump being obviously perceptible and the response amplitude appearing to saturate.

include anatomic factors such as head size, and the geometry/orientation of the neural sources relative to the scalp sensors (Bharadwaj et al., 2019). Thus, although the cortical response to ITD jumps is indeed elicited and parametrically modulated by TFS-based processing, raw response amplitude metrics may be unsuitable for use as an individualized assay of TFS coding.

### Candidate subcortical correlates of TFS processing

Figure 5 shows an example FFR recording from a single individual in response to the stimulus sequence with a probe tone, a forward masker, and a second probe tone. The top row (green traces) shows the differential response across two stimulus polarities. This response to the probe tone (labeled “d1” in Fig. 5) tracks the 500-Hz TFS in the stimulus, but contains both preneural (e.g., CM) and neural components. Because forward masking is thought to arise from synaptic processing (Verschooten and Joris, 2014), the forward masker would be expected to only suppress the neural (i.e., postsynaptic) component of the response to the second probe tone, leaving the preneural component intact (labeled “d2” in Fig. 5). Thus, subtracting d2 from d1 should leave a purely neural response phase-locked to the TFS.

The bottom row in Figure 5, blue traces, shows the summed response across two polarities. Because of inner hair-cell rectification, this response contains a 1000-Hz component arising from the stimulus TFS (also see Materials and Methods). This 1000-Hz component in response to the probe (labeled “s1” in Fig. 5) has previously been interpreted as a neural response (Parthasarathy et al., 2020). If that were indeed the case, the forward-masker would considerably suppress the 1000-Hz

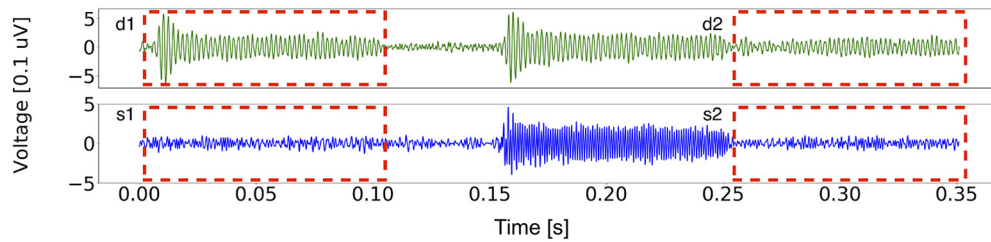


**Figure 5.** FFR to the probe-forward-masker-probe stimulus sequence for an individual subject. The top row (green trace) represents the differential response across two stimulus polarities, whereas the bottom row (blue trace) represents the summed response across two stimulus polarities. The first boxed segments in both rows (red, dashed box, labeled d1 or s1) reflect the raw response to the probe tone, which is likely a mixture of neural and preneural responses (e.g., CM), whereas the second boxed segments in both rows (red, dashed box, labeled d2 or s2) is the adapted response after forward masking. For d2 and s2, the preneural (e.g., CM) component is expected to be intact, whereas the neural response is attenuated by forward masking (because of a very short 1-ms gap). The forward masker only partially suppresses the responses, suggesting a strong preneural contribution to d1 and s1. The weaker residuals obtained by subtraction, i.e., (d1 – d2) and (s1 – s2) are likely purely neural.

component in response to the second probe (labeled “s2” in Fig. 5).

Figure 6 shows the average d1 (Fig. 6A), d1–d2 (Fig. 6B), s1 (Fig. 6C), and s1–s2 (Fig. 6D) response obtained across subjects, quantified in the frequency domain. It is evident from the reduced size of the (d1–d2) response compared with the d1 response, and the reduced size of the (s1–s2) response compared with the s1 response that, forward masker only has a partially suppressing effect. This provides evidence that both candidate TFS measures, the 500-Hz component from the difference across stimulus polarities, and the 1000-Hz component from the sum across stimulus polarities, have significant preneural contributions. This is in contrast to the previous interpretation that the component at double the tone frequency is purely neural (Parthasarathy et al., 2020).

These results indicate that a forward-masking paradigm will need to be employed to extract the purely neural “residual” response. Unfortunately, unlike transtympanic recordings that are difficult to perform (Verschooten et al., 2015), this residual is small and not readily measurable from all individual subjects. Thus, while subcortical envelope-following responses (EFRs) provide a robustly measurable correlate of envelope processing (Bharadwaj et al., 2015), tracking the TFS via FFRs are not promising, and

not readily measured across all individuals despite our cohort being comprised of NH listeners.

#### “Adjusted” behavioral and cortical measures are strongly correlated, likely reflecting TFS coding

Based on individual differences in the cortical amplitude measure persisting for the large-ITD-jump (540  $\mu$ s) condition, we concluded that the amplitude measure of cortical phase-locking was dominated by extraneous variance, likely from anatomic factors. Thus, we focused our attention on the latency of the ITD-jump response, because the latency is expected to be unaffected by the scaling effects of individual anatomy. In particular, we extracted the latency of the cortical response to the 180- $\mu$ s jump condition to avoid floor and ceiling effects. The latency was the mean of N1 and P2 latency (the latency is the time difference between the red dashed line and either N1 or P2 peak in Fig. 1B). The use of the latency metric was also motivated by the previous successful use of this EEG-latency measure to predict individual behavioral measures of spatial release from masking (Papesh et al., 2017). In addition to this latency metric, the slope of the cortical-response amplitude with increasing ITD-jump (i.e., the increase from the 60- $\mu$ s condition to the 180- $\mu$ s condition,

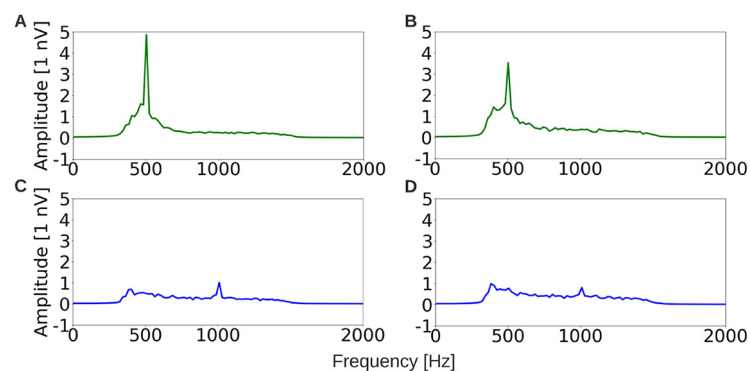


**Figure 6.** Frequency-domain representations of the d1 (A), d1–d2 (B), s1 (C), and s1–s2 (D) segments from Figure 5, but averaged across subjects. Forward masking partially attenuates both the 500-Hz component of d1 response, and the 1000-Hz component of the s1 response, suggesting that both responses reflect a mix of preneural and neural sources.



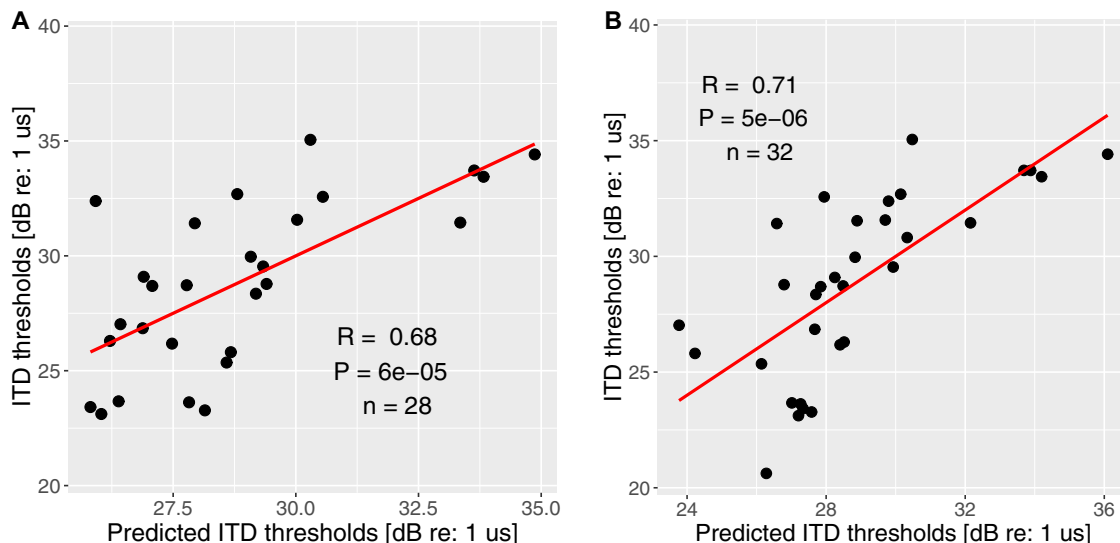


**Figure 7.** Model prediction of the ITD detection thresholds, based on the combination of lapse rate and slope (60- to 180- $\mu$ s condition; **A**), or the combination of lapse rate and EEG latency (**B**). Please refer to [Table 1](#) for the variance explained by each factor.

divided by the 540- $\mu$ s condition, in the ITC plot of [Fig. 4](#)) was extracted as a normalized measure of TFS processing that would mitigate the overall scaling influence of anatomic factors. This normalization was also motivated by the previous successful use of a similarly normalized electrophysiological measure in the context of modulation processing ([Bharadwaj et al., 2015](#)).

Both of these “adjusted” cortical measures exhibited significant correlations with behaviorally measured ITD thresholds. Specifically, individual differences in latency of the cortical ITD-jump response (for 180  $\mu$ s) correlated with individual differences in the ITD detection thresholds ( $R=0.35$ ,  $p=0.048$ ,  $n=32$ ). The correlation improved when the behavioral scores were also adjusted to factor out the nonsensory score ( $R=0.45$ ,  $p=0.01$ ,  $n=32$ ). The slope metric from the cortical EEG response also correlated with ITD thresholds both with and without adjustments to the behavioral scores ( $R=0.43$ ,  $p=0.021$ ,  $n=32$ , original ITD scores;  $R=0.42$ ,  $p=0.028$ , with nonsensory score factored out). There were no significant brain-behavior correlations with “unadjusted” or “raw” metrics, such as the ITC amplitude of the ITD-evoked response, even after normalization by the ITC amplitude of the onset response.

**Table 1: Model prediction of the behavioral ITD detection thresholds, with factors including the nonsensory score, EEG latency, and EEG slope**

Predictor	Variance explained
Nonsensory score	37.48%
EEG latency	10.03%
EEG slope	9.28%
Explained	56.79%
Unexplained	43.21%

The variations accounted for by the nonsensory score are more than three times as by either one of the two EEG metrics. Together, more than half the variance can be explained.

With the subcortical measures, because results indicated a significant preneural contribution for both candidate TFS measures, and the residual neural component extracted from the forward-masking paradigm was not robustly measurable for many participants, we did not explore FFR-behavior associations in detail. A simple correlational analysis between the residual (d1-d2) 500-Hz response and ITD thresholds suggested that the correlations were not statistically distinguishable from zero (data not shown).

A multiple linear regression model was used to predict ITD detection thresholds using both the nonsensory score, the EEG latency, as well as the EEG normalized slope metric (both from cortical ITD-jump response). The model could predict the behavioral ITD threshold well ([Fig. 7](#)) with the predictors together accounting for more than half of the variance observed in the behavioral thresholds ([Table 1](#)). We interpreted this result as suggesting that both “adjusted” behavioral scores, and electrophysiological latency or slope metrics in response to TFS-based binaural processing are promising candidate assays of TFS processing that may be suitable for use at the individual level.

## Discussion

In the present study, we sought to identify viable assays that can index the fidelity of TFS processing at the individual subject level. To obtain insight into whether individual differences in various candidate measures reflected TFS-based processing or extraneous factors, we compared individual differences in behavioral scores across FM and ITD detection tasks to differences in cortical and subcortical EEG-based measures. Results revealed the strong influence of extraneous factors on both behavioral scores and amplitude-based EEG metrics.

With behavioral measures, nonsensory factors quantified using the lapse rate in catch trials, could account for

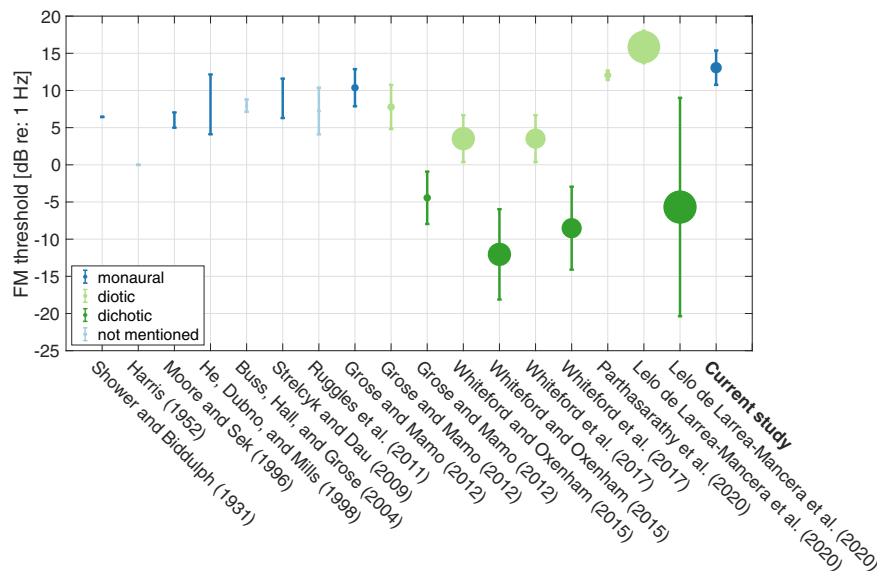


**Figure 8.** A sample of published reports of FM detection thresholds for comparison (Shower and Biddulph, 1931; Harris, 1952; Moore and Sek, 1996; He et al., 1998; Buss et al., 2004; Strelcyk and Dau, 2009; Ruggles et al., 2011; Grose and Mamo, 2012; Whiteford and Oxenham, 2015; Whiteford et al., 2017; Parthasarathy et al., 2020; Lelo de Larrea-Mancera et al., 2020). Error bar is 1 SD. The size of the dot represents the number of subjects (Whiteford and Oxenham (2015) has the most subjects;  $N=100$ ). Stimulus parameters such as stimulus level, carrier frequency, and modulation frequency in the cited studies are similar to those used in the current study, with slight differences (Strelcyk and Dau, 2009; Ruggles et al., 2011, used carrier at 750 Hz). Some threshold values are approximate from figures [e.g., mean and SD had to be estimated based on median and range in the box whisker plots in Whiteford and Oxenham (2015) and Whiteford et al. (2017)]. The mean and SD from the young and middle-aged group from Grose and Mamo (2012) were combined to generate a single data point. Some authors expressed the threshold in terms of  $\Delta F/F_c$ , where  $\Delta F$  is frequency deviation, and  $F_c$  is the carrier frequency. Moore and Sek (1996) used  $\Delta F$  that was in two directions, i.e., peak-peak. Subjects from some studies were highly experienced in psychoacoustic tasks hence the thresholds were very low/good. Whiteford and Oxenham (2015) and Whiteford et al. (2017) obtained thresholds that fall in the lower end of the results of the current study from a very large number of subjects. This may be because their subjects were younger NH listeners and the stimuli were presented diotically and dichotically instead of monaurally.

a third of the variance across individuals. Although previous work has explored a range of behavioral TFS measures (Moore and Sek, 2009; Hopkins and Moore, 2010; Seök and Moore, 2012), the results from the present study underscore the importance of adjusting raw behavioral scores to reduce the impact of nonsensory factors. Indeed, although raw FM and ITD measures correlated significantly with each other, similar to the correlation between monaural AM detection and binaural envelope-ITD thresholds (Bharadwaj et al., 2015), this was driven in part by nonsensory factors. Because phase-locking to the TFS is essential for low-frequency ITD processing (Yin and Chan, 1990), it is plausible that ITD detection thresholds can provide an index of TFS sensitivity. On the other hand, whether FM detection relies on TFS coding has been controversial because of the possible role of recovered ENV cues that result from cochlear filtering of FM stimuli; indeed, FM stimuli lead to perceptible out-of-phase ENV fluctuations at cochlear places tuned to frequencies just above and below the FM carrier (Whiteford and Oxenham, 2015; Whiteford et al., 2017). Whiteford et al. (2020) extensively tested the role of place coding in FM detection and found that place coding by itself can account for the observed variations in FM sensitivity across all carrier frequencies and modulation rates. This finding is in contrast to the widely accepted view of the utilization

of time coding in the detection of slow-rate FM (Moore and Sek, 1996; Strelcyk and Dau, 2009; Parthasarathy et al., 2020). Together with our finding that nonsensory factors influence raw behavioral scores, this uncertainty about the link between TFS coding and FM detection calls into question the previous use of FM detection scores as a correlate of TFS processing. In contrast, unambiguous theoretical links can be made between ITD detection and TFS coding, suggesting that once ITD thresholds are adjusted to reduce the influence of nonsensory scores, they may serve as a useful metric of TFS processing. This was corroborated by our finding that passive EEG measures, when combined with nonsensory scores, can account for more than half of the variance in ITD thresholds. Here, we used lapse rates in the catch trials to obtain a correlate of nonsensory factors. Alternately, a surrogate behavioral task that does not rely on TFS coding (e.g., interaural level difference sensitivity) may also be used to adjust ITD thresholds with similar benefits.

Another key finding from the present study is that although passive EEG measurements can potentially reflect TFS-based processing objectively, they too are susceptible to the influence of extraneous factors. Indeed, consistent with the interpretation that individual anatomic factors can have a scaling influence on response

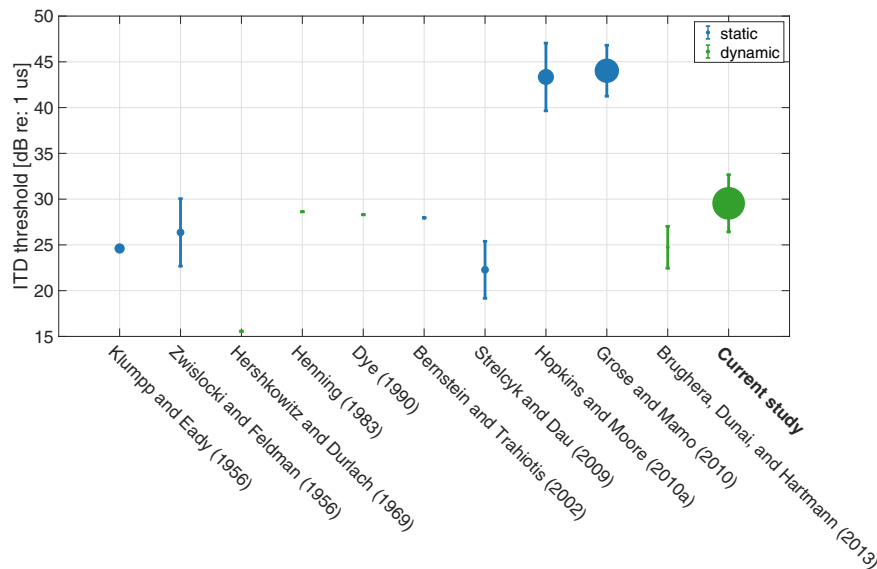


**Figure 9.** A sample of published reports of ITD detection thresholds for comparison (Klumpp and Eady, 1956; Zwicker, 1956; Hershkowitz and Durlach, 1969; Henning, 1983; Dye, 1990; Bernstein and Trahiotis, 2002; Strelcyk and Dau, 2009; Hopkins and Moore, 2010; Grose and Mamo, 2010; Brughera et al., 2013). Error bar is 1 SD. The size of the dot represents the number of subjects (the current study has the most subjects;  $N = 36$ ). Stimulus parameters such as level and carrier frequency in the cited studies are similar to those used in the current study, with slight differences [Strelcyk and Dau (2009) used carrier at 750 Hz]. Note that some threshold values were extracted approximately from figures rather than direct numerical reports. Some of the studies used stimuli with the leading ear switching from one side to the other (labeled “dynamic,” marked in green color), whereas others presented an ITD only in the target intervals, with the reference being the midline (labeled “static,” marked in blue color). Note that the values from Hershkowitz and Durlach (1969) and Brughera et al. (2013) were halved since the authors used  $ITD/2$  in each interval. The mean and SD from young and middle-aged cohort from Grose and Mamo (2010) were combined to generate a single data point. Subjects from some studies were highly experienced in psychoacoustic tasks.

amplitudes, we found that cortical responses phase-locked to ITD changes showed large individual differences even for a large ITD jump ( $540 \mu\text{s}$ ) where the response amplitude was near saturation for most individuals. Therefore, we argued that the evoked-response latency and/or percent growth/slope metrics may be better assays of TFS processing. Accordingly, latency and slope metrics showed significant correlations with behavioral ITD detection thresholds. For candidate subcortical FFR-based measures of TFS processing, our results showed that preneural physiological currents (CM, inner hair-cell currents) contribute significantly to the measure, thus complicating their applicability. Indeed, brainstem response measures from individuals with compromised inner hair-cell synaptic transmission show that preneural transduction currents can contribute to the measured response (Santarelli et al., 2009). Moreover, when employing a forward-masking-based design to isolate the neural component of the FFR, the resulting signal is relatively weak even in our NH cohort. This result from non-invasive ear-canal recordings is in contrast to neurophonic measurements from the auditory nerve (Snyder and Schreiner, 1985) or round window (Henry, 1995) from animals, or FFR measurements from humans using transtympanic electrodes where the forward-masking design has been used successfully (Verschooten et al., 2018). Although FFRs have previously been used as a putative correlate of TFS-based processing (Parthasarathy et al., 2020), our results suggest that additional experiments are needed to clarify the interpretation of those results.

Our finding that the subcortical FFR may be a poor correlate of neural TFS processing is in contrast to previous results suggesting that subcortical EFRs are correlated with behavioral measures of ENV processing. For example, Bharadwaj et al. (2015) showed that the AM detection thresholds and ENV-based ITD thresholds correlated strongly with normalized EFR-based metrics. This is likely both because EFR measurements more readily exclude preneural contributions (which primarily track the TFS), and because Bharadwaj et al. (2015) obtained asymptotic behavioral scores from a large number of trials (1200–1500 trials) from trained subjects. Indeed, with naive subjects in this study, an AM detection task similar to the one used in Bharadwaj et al. (2015) also showed a strong influence of nonsensory factors.

In summary, the present study examined various candidate assays for quantifying TFS processing at the individual subject level. These included behavioral FM and ITD detection thresholds, and EEG-based cortical and subcortical physiological measures. Among these, our experiments suggest that the latency of cortical responses to ITD jumps, normalized cortical response amplitude (i.e., percent growth/slope), and “adjusted” ITD thresholds may all be useful. Indeed, when a multiple linear regression model was constructed to predict behavioral ITD thresholds, the combination of the nonsensory score (lapse rate in catch trials), EEG latency, and slope measures could account for  $>50\%$  of the variance across individuals. Our results are consistent with the findings by

Papesh et al. (2017), who also found a correlation between ITD-evoked EEG latency and spatial-hearing outcomes such as spatial release from masking. Given that multiple candidate measures were explored to identify the most promising assays, future experiments should be conducted to independently confirm the efficacy of the assays endorsed by our results. The most promising assays rely on binaural TFS-based processing. Indeed, similarly to our results, steady-state cortical responses that track continuous interaural phase modulations have also been found to correlate with behavioral binaural sensitivity, further corroborating the potential utility of cortical binaural measures as electrophysiological assays of TFS processing (Undurraga et al., 2016; Koerner et al., 2020).

Reliable measures of TFS processing are critical for future investigations into the role of TFS in everyday hearing using intact speech-in-noise stimuli without vocoding manipulations. While sub-band vocoding can allow for independent manipulation of acoustic TFS and envelope cues, subsequent cochlear processing can confound these factors once again (Gilbert and Lorenzi, 2006; Swaminathan and Heinz, 2012). Furthermore, when both rate-place/ENV cues and TFS cues are redundant, vocoding experiments cannot provide insight into how they are perceptually weighted. The candidate TFS measures identified in the present study can help address these gaps.

## References

- Ardoit M, Lorenzi C (2010) Effects of lowpass and highpass filtering on the intelligibility of speech based on temporal fine structure or envelope cues. *Hear Res* 260:89–95.
- Benjamini Y, Hochberg Y (1995) Controlling the false discovery rate: a practical and powerful approach to multiple testing. *J R Stat Soc Series B Stat Methodol* 57:289–300.
- Bernstein LR, Trahiotis C (2002) Enhancing sensitivity to interaural delays at high frequencies by using “transposed stimuli.” *J Acoust Soc Am* 112:1026–1036.
- Bernstein JG, Oxenham AJ (2003) Pitch discrimination of diotic and dichotic tone complexes: harmonic resolvability or harmonic number? *J Acoust Soc Am* 113:3323–3334.
- Best V, Ozmeral E, Gallun FJ, Sen K, Shinn-Cunningham BG (2005) Spatial unmasking of birdsong in human listeners: energetic and informational factors. *J Acoust Soc Am* 118:3766–3773.
- Bharadwaj HM, Shinn-Cunningham BG (2014) Rapid acquisition of auditory subcortical steady-state responses using multichannel recordings. *Clin Neurophysiol* 125:1878–1888.
- Bharadwaj HM, Masud S, Mehraei G, Verhulst S, Shinn-Cunningham BG (2015) Individual Differences Reveal Correlates of Hidden Hearing Deficits. *J Neurosci* 35:2161–2172.
- Bharadwaj HM, Mai AR, Simpson JM, Choi I, Heinz MG, Shinn-Cunningham BG (2019) Non-invasive assays of cochlear synaptopathy—candidates and considerations. *Neuroscience* 407:53–66.
- Brughera A, Dunai L, Hartmann WM (2013) Human interaural time difference thresholds for sine tones: the high-frequency limit. *J Acoust Soc Am* 133:2839–2855.
- Buss E, Hall JWI, Grose JH (2004) Temporal fine-structure cues to speech and pure tone modulation in observers with sensorineural hearing loss. *Ear Hear* 25:242–250.
- Drullman R (1995) Temporal envelope and fine structure cues for speech intelligibility. *J Acoust Soc Am* 97:585–592.
- Dye RH (1990) The combination of interaural information across frequencies: lateralization on the basis of interaural delay. *J Acoust Soc Am* 88:2159–2170.
- Gilbert G, Lorenzi C (2006) The ability of listeners to use recovered envelope cues from speech fine structure. *J Acoust Soc Am* 119:2438–2444.
- Glasberg BR, Moore BCJ (1990) Derivation of auditory filter shapes from notched-noise data. *Hear Res* 47:103–138.
- Grose JH, Mamo SK (2010) Processing of temporal fine structure as a function of age. *Ear Hear* 31:755–760.
- Grose JH, Mamo SK (2012) Frequency modulation detection as a measure of temporal processing: age-related monaural and binaural effects. *Hear Res* 294:49–54.
- Harris JD (1952) Pitch discrimination. *J Acoust Soc Am* 24:750–755.
- Hasenstaub A, Otte S, Callaway E, Sejnowski TJ (2010) Metabolic cost as a unifying principle governing neuronal biophysics. *Proc Natl Acad Sci USA* 107:12329–12334.
- He NJ, Dubno JR, Mills JH (1998) Frequency and intensity discrimination measured in a maximum-likelihood procedure from young and aged normal-hearing subjects. *J Acoust Soc Am* 103:553–565.
- Henning GB (1983) Lateralization of low-frequency transients. *Hear Res* 9:153–172.
- Henry KR (1995) Auditory nerve neurophonic recorded from the round window of the Mongolian gerbil. *Hear Res* 90:176–184.
- Hershkowitz RM, Durlach NI (1969) Interaural time and amplitude jnds for a 500-Hz tone. *J Acoust Soc Am* 46:1464–1467.
- Hilbert D (1906) Grundzüge einer allgemeinen Theorie der linearen Integralgleichungen. Vierte Mitteilung. Nachrichten von der Gesellschaft der Wissenschaften zu Göttingen, Mathematisch-Physikalische Klasse 1906:157–228.
- Hopkins K, Moore BCJ (2009) The contribution of temporal fine structure to the intelligibility of speech in steady and modulated noise. *J Acoust Soc Am* 125:442–446.
- Hopkins K, Moore BCJ (2010) Development of a fast method for measuring sensitivity to temporal fine structure information at low frequencies. *Int J Audiol* 49:940–946.
- Hopkins K, Moore BCJ, Stone MA (2008) Effects of moderate cochlear hearing loss on the ability to benefit from temporal fine structure information in speech. *J Acoust Soc Am* 123:1140–1153.
- Houtsma AJ, Smurzynski J (1990) Pitch identification and discrimination for complex tones with many harmonics. *J Acoust Soc Am* 87:304–310.
- Ihlefeld A, Shinn-Cunningham BG (2011) Effect of source spectrum on sound localization in an everyday reverberant room. *J Acoust Soc Am* 130:324–333.
- Johnson DH (1980) The relationship between spike rate and synchrony in responses of auditory-nerve fibers to single tones. *J Acoust Soc Am* 68:1115–1122.
- Joris PX, Yin TC (1992) Responses to amplitude-modulated tones in the auditory nerve of the cat. *J Acoust Soc Am* 91:215–232.
- Joris P, Schreiner C, Rees A (2004) Neural processing of amplitude-modulated sounds. *Physiol Rev* 84:541–578.
- Kaernbach C (1991) Simple adaptive testing with the weighted up-down method. *Percept Psychophys* 49:227–229.
- Kidd G, Watson C, Gygi B (2007) Individual differences in auditory abilities. *J Acoust Soc Am* 122:418–435.
- Klumpp RG, Eady HR (1956) Some measurements of interaural time difference thresholds. *J Acoust Soc Am* 28:859–860.
- Koerner TK, Muralimanohar RK, Gallun FJ, Billings CJ (2020) Age-related deficits in electrophysiological and behavioral measures of binaural temporal processing. *Front Neurosci* 14:578566.
- Laughlin SB, de Ruyter van Steveninck RR, Anderson JC (1998) The metabolic cost of neural information. *Nat Neurosci* 1:36–41.
- Lelo de Larrea-Mancera ES, Stavropoulos T, Hoover EC, Eddins DA, Gallun FJ, Seitz AR (2020) Portable automated rapid testing (PART) for auditory assessment: validation in a young adult normal-hearing population. *J Acoust Soc Am* 148:1831–1851.
- Lorenzi C, Debrulle L, Garnier S, Fleuriot P, Moore BCJ (2009) Abnormal processing of temporal fine structure in speech for frequencies where absolute thresholds are normal. *J Acoust Soc Am* 125:27–30.

- McDermott JH, Lehr AJ, Oxenham AJ (2010) Individual differences reveal the basis of consonance. *Curr Biol* 20:1035–1041.
- Metting van Rijn A, Peper A, Grimbergen C (1990) High-quality recording of bioelectric events. *Med Biol Eng Comput* 28:389–397.
- Moore BC (1973) Frequency difference limens for short-duration tones. *J Acoust Soc Am* 54:610–619.
- Moore BC (1986) Parallels between frequency selectivity measured psychophysically and in cochlear mechanics. *Scand Audiol Suppl* 25:139–152.
- Moore BCJ, Sek A (1996) Detection of frequency modulation at low modulation rates: evidence for a mechanism based on phase locking. *J Acoust Soc Am* 100:2320–2331.
- Moore BCJ, Sek A (2009) Development of a fast method for determining sensitivity to temporal fine structure. *Int J Audiol* 48:161–171.
- Oxenham AJ (2012) Pitch perception. *J Neurosci* 32:13335–13338.
- Oxenham AJ (2013) Revisiting place and temporal theories of pitch. *Acoust Sci Technol* 34:388–396.
- Oxenham AJ, Simonson AM (2009) Masking release for low-and high-pass-filtered speech in the presence of noise and single-talker interference. *J Acoust Soc Am* 125:457–468.
- Papesh MA, Folmer RL, Gallun FJ (2017) Cortical measures of binaural processing predict spatial release from masking performance. *Front Hum Neurosci* 11:124.
- Parthasarathy A, Hancock KE, Bennett K, DeGruttola V, Polley DB (2020) Bottom-up and top-down neural signatures of disordered multi-talker speech perception in adults with normal hearing. *Elife* 9:e51419.
- Picton TW, John MS, Dimitrijevic A, Purcell D (2003) Human auditory steady-state responses: respuestas auditivas de estado estable en humanos. *Int J Audiol* 42:177–219.
- Ruggles D, Bharadwaj H, Shinn-Cunningham BG (2011) Normal hearing is not enough to guarantee robust encoding of suprathreshold features important in everyday communication. *Proc Natl Acad Sci USA* 108:15516–15521.
- Santarelli R, Del Castillo I, Rodríguez-Ballesteros M, Scimemi P, Cama E, Arslan E, Starr A (2009) Abnormal cochlear potentials from deaf patients with mutations in the otoferlin gene. *J Assoc Res Otolaryngol* 10:545–556.
- Sek A, Moore BCJ (2012) Implementation of two tests for measuring sensitivity to temporal fine structure. *Int J Audiol* 51:58–63.
- Showers EG, Biddulph R (1931) Differential pitch sensitivity of the ear. *J Acoust Soc Am* 3:275–287.
- Smith ZM, Delgutte B, Oxenham AJ (2002) Chimaeric sounds reveal dichotomies in auditory perception. *Nature* 416:87–90.
- Snyder RL, Schreiner CE (1985) Forward masking of the auditory nerve neurophonic (ANN) and the frequency following response (FFR). *Hear Res* 20:45–62.
- Strelcyk O, Dau T (2009) Relations between frequency selectivity, temporal fine-structure processing, and speech reception in impaired hearing. *J Acoust Soc Am* 125:3328–3345.
- Swaminathan J, Heinz MG (2012) Psychophysiological analyses demonstrate the importance of neural envelope coding for speech perception in noise. *J Neurosci* 32:1747–1756.
- Undurraga JA, Haywood NR, Marquardt T, McAlpine D (2016) Neural representation of interaural time differences in humans—an objective measure that matches behavioural performance. *J Assoc Res Otolaryngol* 17:591–607.
- Uusitalo MA, Ilmoniemi RJ (1997) Signal-space projection method for separating MEG or EEG into components. *Med Biol Eng Comput* 35:135–140.
- Verschouten E, Joris PX (2014) Estimation of neural phase locking from stimulus-evoked potentials. *J Assoc Res Otolaryngol* 15:767–787.
- Verschouten E, Robles L, Joris PX (2015) Assessment of the limits of neural phase-locking using mass potentials. *J Neurosci* 35:2255–2268.
- Verschouten E, Desloovere C, Joris PX (2018) High-resolution frequency tuning but not temporal coding in the human cochlea. *PLoS Biol* 16:e2005164.
- Verschouten E, Shamma S, Oxenham AJ, Moore BCJ, Joris PX, Heinz MG, Plack CJ (2019) The upper frequency limit for the use of phase locking to code temporal fine structure in humans: a compilation of viewpoints. *Hear Res* 377:109–121.
- Viemeister NF (1979) Temporal modulation transfer functions based upon modulation thresholds. *J Acoust Soc Am* 66:1364–1380.
- Viswanathan V, Bharadwaj HM, Shinn-Cunningham BG, Heinz MG (2021) Modulation masking and fine structure shape neural envelope coding to predict speech intelligibility across diverse listening conditions. *J Acoust Soc Am* 150:2230–2244.
- Whiteford KL, Oxenham AJ (2015) Using individual differences to test the role of temporal and place cues in coding frequency modulation. *J Acoust Soc Am* 138:3093–3104.
- Whiteford KL, Kreft HA, Oxenham AJ (2017) Assessing the role of place and timing cues in coding frequency and amplitude modulation as a function of age. *J Assoc Res Otolaryngol* 18:619–633.
- Whiteford KL, Kreft HA, Oxenham AJ (2020) The role of cochlear place coding in the perception of frequency modulation. *Elife* 9:e58468.
- Yin TC, Chan JC (1990) Interaural time sensitivity in medial superior olive of cat. *J Neurophysiol* 64:465–488.
- Zwicker E (1956) Die elementaren Grundlagen zur Bestimmung der Informationskapazität des Gehörs. *Acta Acustica united with Acustica* 6:365–381.